

University of Nebraska - Lincoln

DigitalCommons@University of Nebraska - Lincoln

---

P. F. (Paul Frazer) Williams Publications

Electrical & Computer Engineering, Department of

---

January 1987

# Field-enhancement calculations for a field-distortion triggered spark gap

B. Pashale

*Texas Tech University, Lubbock, TX*

G. Schaefer

*Texas Tech University, Lubbock, TX*

K. H. Schoenbach

*Texas Tech University, Lubbock, TX*

P. F. Williams

*University of Nebraska - Lincoln, pfw@moi.unl.edu*

Follow this and additional works at: <http://digitalcommons.unl.edu/elecengwilliams>



Part of the [Electrical and Computer Engineering Commons](#)

---

Pashale, B.; Schaefer, G.; Schoenbach, K. H.; and Williams, P. F., "Field-enhancement calculations for a field-distortion triggered spark gap" (1987). *P. F. (Paul Frazer) Williams Publications*. 21.  
<http://digitalcommons.unl.edu/elecengwilliams/21>

This Article is brought to you for free and open access by the Electrical & Computer Engineering, Department of at DigitalCommons@University of Nebraska - Lincoln. It has been accepted for inclusion in P. F. (Paul Frazer) Williams Publications by an authorized administrator of DigitalCommons@University of Nebraska - Lincoln.

# Field-enhancement calculations for a field-distortion triggered spark gap

B. Pashaie, G. Schaefer,<sup>a)</sup> and K. H. Schoenbach<sup>b)</sup>

Department of Electrical Engineering, Texas Tech University, Lubbock, Texas 79409-4439

P. F. Williams

Department of Electrical Engineering, University of Nebraska-Lincoln, Lincoln, Nebraska 68588-0511

(Received 5 June 1986; accepted for publication 1 October 1986)

We present the results of numerical field calculation which supplement a recent article in which we described a new design concept for field-distortion triggered spark gaps. The calculations verify the shielding and field enhancement assumptions made in the article, and they provide insight into the interaction of the design tradeoffs associated with simultaneously maximizing the holdoff voltage and the triggering capability of the gap.

Recently we described a new design concept for field-distortion triggered spark gaps.<sup>1</sup> Briefly, the design consisted of a pointed main gap electrode shielded in the untriggered state by the trigger electrode as shown in Fig. 1. Triggering was accomplished by changing the potential of the trigger electrode from that of the nearby pointed electrode to that of the opposite main gap electrode. In this configuration a very high field is generated at the tip of the pointed main gap electrode, causing large field enhancements and rapid breakdown of the main gap. We also reported the results of proof-of-concept experiments which demonstrated the validity of the design. With a simple switch we obtained a closing delay of  $\sim 10$  ns, with a jitter of  $\sim 2$  ns, for charging voltages of 90% of the static, self-breakdown voltage,  $V_{SB}$ .

We have extended this work by calculating numerically the electric field for a gap geometry similar to that we reported on earlier. These calculations verify the shielding of the pointed electrode by the trigger electrode and the sensitivity of this shielding to the position of the trigger electrode. The calculations also verify the presence of very high field enhancements in the triggered state. In this communication we present the results of these calculations and discuss their application to the design of field-distortion triggered spark gaps such as we described previously.

The numerical code we used for the field calculations was written by researchers associated with the Tetra Corporation, Albuquerque, NM, for analyzing the field distribution in discharges for lasers and switches.<sup>2,3</sup> Briefly, the code operates by determining a set of boundary-fitted coordinates which match the given boundary value surfaces. Laplace's equation for the electrostatic potential is then solved in these coordinates using a successive over-relaxation technique, and the electric field is determined by taking the gradient of this potential numerically. Although the configuration of interest here contains three electrode surfaces, the potential of two of these surfaces is the same in the two states of interest (holdoff and triggered) so that the boundary condition specification for the code consisted of two surfaces, one surface in each case containing two electrodes.

Figure 2 shows the electrode geometry used in these calculations. The gap is taken to have cylindrical symmetry, and the figure shows a cross section containing the gap axis. The experiments we reported utilized a linear rather than cylindrical geometry, but the fields in the two cases should be similar. The gap field was calculated using the code for both the holdoff and the triggered cases for a number of positions of the triggered electrode. In either case, the trigger electrode was connected to one of the main gap electrodes. A  $17 \times 17$  element grid mesh was used in the calculations.

Figures 3(a) and 3(b) show the equipotential lines for the holdoff and triggered cases, respectively, for a particular positioning of the trigger electrode corresponding to the maximum field enhancement factor at the tip of the pointed electrode. The efficiency of the shielding of the pointed electrode by the trigger electrode in the untriggered state is apparent in Fig. 3(a), where the field is seen to be reasonably uniform throughout the gap region, with no field enhancement in the vicinity of the pointed electrode. In the triggered state, on the other hand, shown in Fig. 3(b), the field is highly nonuniform, with large fields appearing near the tip of the pointed electrode. In this case the maximum field is of the order of 100 times the uniform field value. Corona and other phenomena associated with high overvoltages would be expected to appear promptly at the electrode tip with triggering.

We can define a field enhancement factor  $\beta$  as the ratio of the maximum field at the surface of an electrode,  $E_{max}$ , to the mean field in the gap,  $\langle E \rangle$ ,  $\beta = E_{max} / \langle E \rangle$ . Figures 4(a)

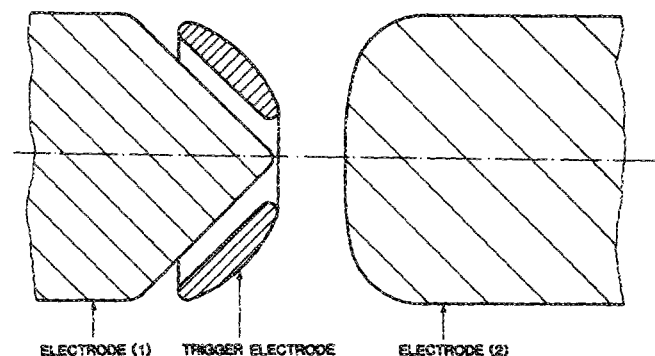


FIG. 1. Schematic drawing of the triggering concept discussed in Ref. 1.

<sup>a)</sup> Present address: Department of Electrical Engineering, Polytechnic University of New York, Farmingdale, NY 11735.

<sup>b)</sup> Present address: Department of Electrical Engineering, Old Dominion University, Norfolk, VA 23508.

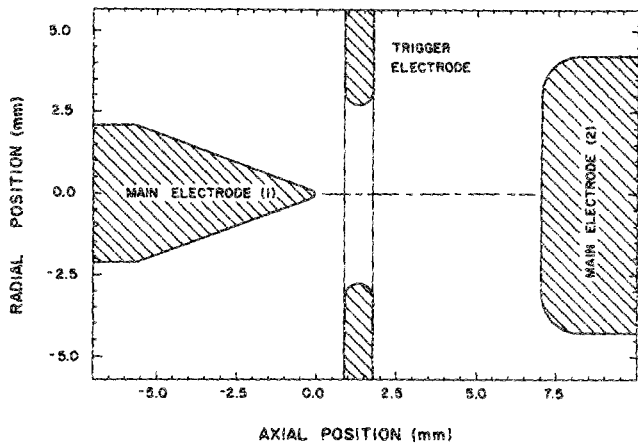


FIG. 2. Drawing showing the electrode geometry used in the calculations reported here.

and 4(b) show  $\beta$  at both the pointed main gap electrode and the trigger electrode as a function of trigger electrode position in the holdoff and triggered states, respectively. In these figures the position refers to the center plane of the trigger electrode. When the trigger electrode is placed well behind the tip of the pointed electrode, we see that the field enhancement factor  $\beta$  in the holdoff state [Fig. 4(a)] reaches a value of  $\sim 6$ , which corresponds to the field enhancement of the bare, unshielded, pointed electrode. For trigger electrode

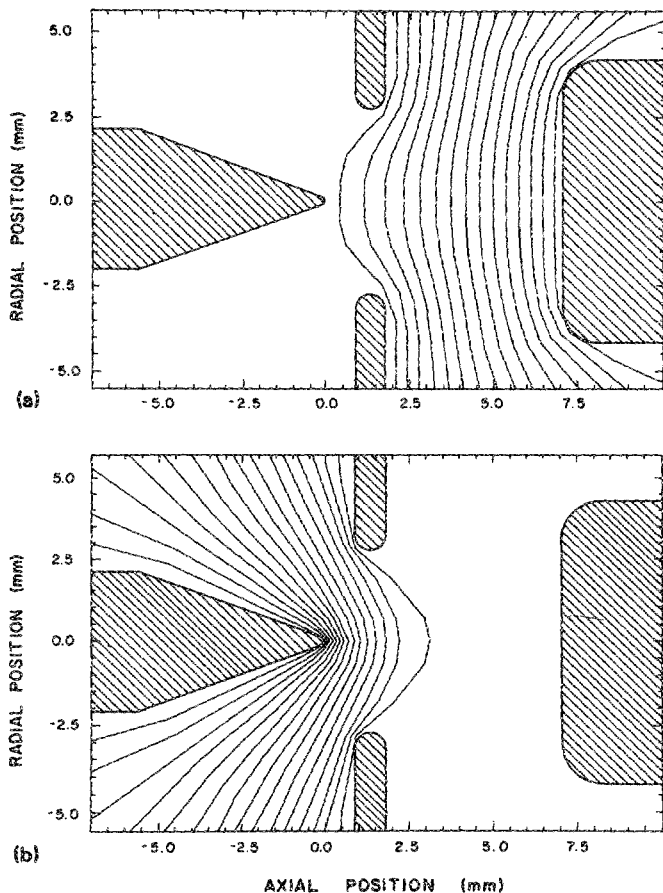


FIG. 3. Plots showing the calculated equipotentials for the spark gap. The position refers to the center plane of the trigger electrode. (a) Holdoff state. (b) Triggered state.

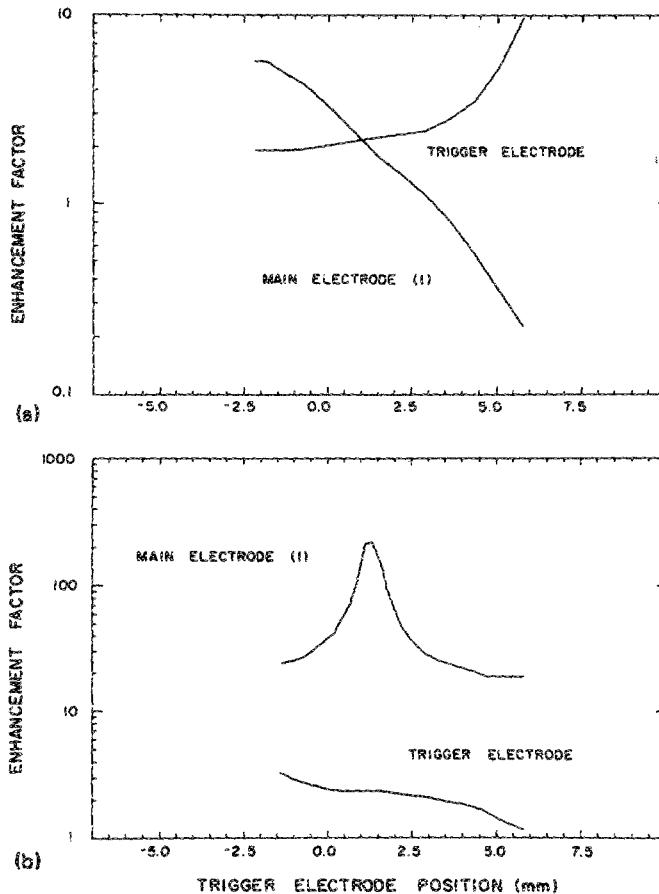


FIG. 4. Plots showing the maximum field enhancement factor at the pointed electrode and the triggered electrode as a function of the position of the center plane of the trigger electrode. (a) Holdoff state. (b) Triggered state.

positioning just in front of the adjacent main electrode point, the field enhancement factor falls to nearly unity, indicating that the holdoff voltage of the gap will be comparable to that of the uniform field gap. Figure 4(b) shows that in the triggered state the maximum field enhancement at the main gap electrode peaks sharply for a trigger electrode position about 1.2 mm in front of the main electrode tip. For this design the trigger electrode position for maximum triggered state enhancement is nearly the same as the position for minimum holdoff state enhancement, a desirable condition for achieving maximum holdoff voltage with maximum triggering capability.

In the experimental work we previously reported,<sup>1</sup> we found that the breakdown voltage in the untriggered state was a strong function of the position of the trigger electrode, peaking sharply at a position just in front of the main electrode point. In order to compare this empirical result with our field calculation results, we assume that the breakdown condition is determined by the maximum field found anywhere in the gap. Thus, the ratio of the actual breakdown voltage to the breakdown voltage of a comparable uniform field gap will be proportional to the inverse of the field enhancement factor,  $1/\beta$ . In Fig. 5 we show  $1/\beta$  and the empirically determined breakdown voltage, both normalized with respect to the maximum value in the untriggered case, plotted against trigger electrode position. The results are similar in both the experimental and theoretical cases. There

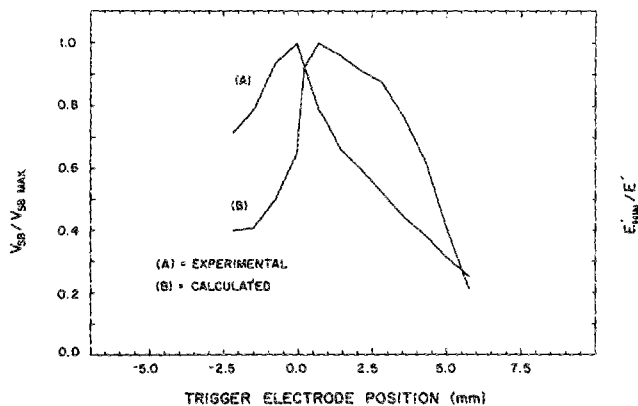


FIG. 5. Plots comparing the numerical estimates with experimental results for the maximum holdoff voltage in the untriggered state as a function of trigger electrode position. (a) Experimental results from Ref. 1 plotted normalized to the maximum holdoff voltage observed. (b) Plots of the inverse of the maximum field anywhere in the gap ( $E'$ ) as a function of electrode position, normalized to the minimum value of  $E'$  ( $E'_{MIN}$ ). In the simple model discussed in the text, the trigger electrode position producing  $E'_{MIN}$  should produce  $V_{SB\ MAX}$ .

is a small difference in the position of the maximum breakdown voltage and the minimum field enhancement factor, but such a difference is not surprising in light of the difference between the geometries in the experiment and calculation, and the simplicity of the assumption that the breakdown voltage is determined solely by the maximum value of the field anywhere in the gap.

We have shown that with proper understanding of the physical mechanisms involved in the triggered breakdown of spark gaps, new and potentially improved designs for these devices can be generated. Clearly, more experimental work

is required to refine and determine the limits of the design concept we proposed earlier.<sup>1</sup> Of perhaps more importance, however, is the development of understanding of the triggered breakdown process itself in these gaps. We believe that breakdown is initiated by the creation of a streamer in the highly field-enhanced region just outside the pointed main gap electrode which then propagates across the gap. Very little quantitative information is available, however, about the propagation of streamers in such highly nonuniform fields. Even less is known about the propagation of these streamers in the substantially reduced field present in the gap between the trigger and the opposite main gap electrodes. It is quite possible that an optimum design would involve setting the trigger electrode potential at some value between the potentials of the two main gap electrodes in the triggered state, or using a selected trigger pulse length in order to provide high fields for streamer initiation, but then to provide a field near the uniform field value for propagation across the main gap.

The authors are grateful to Dr. W. Mooney and Dr. M. von Dodelszen of Tetra Corporation for making the field calculator code available to us and for helpful comments and advice on using it. This work was jointly supported by AFOSR and ARO.

<sup>1</sup>G. Schaefer, B. Pashaie, P. F. Williams, K. H. Schoenbach, and H. Krompholz, *J. Appl. Phys.* **57**, 2507 (1985).

<sup>2</sup>P. J. Roache, W. M. Moeny, and J. A. Filcoff, in *Proceedings of the 3rd IEEE Pulsed Power Conference, Albuquerque, NM*, edited by T. H. Martin and A. H. Guenther (Texas Tech Press, Lubbock, 1981), p. 282.

<sup>3</sup>P. J. Roache, H. J. Happ, and W. M. Moeny, in *Proceedings of the 4th IEEE Pulsed Power Conference, Albuquerque, NM*, edited by T. H. Martin and M. F. Rose (Texas Tech Press, Lubbock, 1983), p. 426.

## The effect of nitrogen implantations on A15 phase formation in $Nb_3Si$

Mireille Treuil Clapp

*Mechanical Engineering Department, University of Massachusetts, Amherst, Massachusetts 01003*

Tariq Manzur

*Metallurgy Department, University of Connecticut, Storrs, Connecticut 06268*

(Received 7 August 1986; accepted for publication 30 September 1986)

Amorphous ribbons of  $Nb_{79}Si_{21}$  were formed using the melt spinning technique. These were then implanted with nitrogen ions to form uniform surface layers of 1 and 2 at. % N. The A15 phase formed between annealing temperatures of 650–750 °C. The lattice parameter was 0.514 nm and the superconducting transition temperature was 6 K. To our knowledge, previous attempts to synthesize A15  $Nb_3Si$  from amorphous solids have required the application of very high pressures.

Many advances in superconductivity materials research involve novel processing techniques of A15 compounds. This particular crystal structure can have very high values of the critical superconducting parameters, temperature  $T_c$ ,

current density  $J_c$ , and magnetic field  $H_c$ . Unfortunately, A15's have very poor mechanical properties and are extremely brittle. We have discovered a technique for processing flexible A15 tapes with unusually high  $J_c$ 's and  $H_c$ 's.<sup>1-3</sup>